Evolutionary Periodogram for Nonstationary Signals

A. Salim Kayhan, *Member, IEEE*, Amro El-Jaroudi, *Member, IEEE*, and Luis F. Chaparro, *Senior Member, IEEE*

***Abstract*—In this paper, we present a novel estimator for the time-dependent spectrum of a nonstationary signal. By modeling the signal, at any given frequency, as having a time-varying amplitude accurately represented by an orthonormal basis expansion, we are able to compute a minimum mean-squared error estimate of this time-varying amplitude. Repeating the process over all frequencies, we obtain a power distribution as a function of time and frequency that is consistent with the Wold-Cramer evolutionary spectrum. Based on the model assumptions, we develop the evolutionary periodogram (EP) for nonstationary signals, an estimator analogous to the periodogram used in the stationary case. We also derive the time-frequency resolution of the new estimator. Our approach is free of some of the drawbacks of the bilinear distributions and of the short-time Fourier transform spectral estimates. It is guaranteed to produce nonnegative spectra without the cross-term behavior of the bilinear distributions, and it does not require windowing of data in the time domain. Examples illustrating the new estimator are given.**

I. Introduction

SINCE most temporal signals of interest (e.g., speech, seismic and biomedical signals) display some kind of nonstationarity, the spectral analysis of such signals is a topic of great research interest. Spectral analysis of nonstationary signals has been usually done assuming local stationarity or slow variation of the statistics of the signal. Differently from the spectral analysis of stationary signals, related to power distribution over frequency, there is no unique definition of the time-dependent spectrum for nonstationary signals. In all cases, however, such definitions must posses certain properties which are verified when, in particular, the process is stationary [1].

Presently, there are three main approaches to the estimation of time-dependent spectrum of a nonstationary signal: The short time Fourier transform (STFT) [2], the Wigner distribution [3] and the evolutionary spectrum [4]. Related approaches have also been developed [5]–[7]. The STFT has been used for a number of years in various areas of signal processing [8], [9]. It assumes stationarity of the signal within a temporal window chosen to balance the time-frequency resolution of the spectrum. The most significant drawback of the STFT as an estimator of the time-varying spectrum is the time-frequency resolution trade-off that results from windowing of the signal. This drawback has often been addressed by the use of time-varying windows to achieve the desired frequency resolution at different times [10]. Another procedure for time-varying spectral analysis is the Wigner distribution. Despite the fact it has important and desirable mathematical properties, the Wigner distribution also has significant limitations. The existence of cross-terms, for instance, makes the Wigner distribution difficult to interpret. Moreover, the positivity of the spectral density is not guaranteed. The cross-terms can be reduced by the use of smoothing kernels [6], [7]. Finally, the evolutionary spectrum proposed by Priestley [4] is another approach to the estimation of the time-varying power spectrum of a nonstationary signal. In the evolutionary spectral theory, attention is restricted to a class of processes called oscillatory processes. The spectral estimates are obtained by complex demodulation and lowpass filtering. As a special case of Priestley's evolutionary spectrum, one can obtain Melard's Wold-Cramer evolutionary spectrum [11] by representing the nonstationary process in terms of its innovations. Melard [4], [11] and Tjostheim [4] independently proposed such an approach. With the Wold-Cramer spectrum, one obtains a unique rather than a class of spectral density functions -as is the case in Priestley's evolutionary spectrum- which satisfies the properties in [1].

Parametric approaches to the time-dependent spectral estimation have also been proposed. Rao [12] was the first to consider autoregressive models for nonstationary signals with time-varying coefficients represented as expansions of orthogonal polynomials. Many other researchers [13]–[15] have used this approach. It was shown using this approach that the spectrum of a nonstationary signal cannot be viewed as a concatenation of "frozen-time" spectra [11], [14]. This makes the connection of the time-varying models to the power spectrum difficult to establish.

The rest of the paper is organized as follows. In Section II, we briefly review Melard's Wold-Cramer evolutionary spectrum and use it to propose a model for the frequency components of a nonstationary signal. Then in Section III, we develop a linear minimum mean-squared error estimator for the time-varying amplitude at each frequency. In Section IV, we focus on a time-varying or evolutionary periodogram (EP) estimator which we obtain from the amplitude estimator of Section III, and discuss some of its properties. The time-frequency resolution, the filtering interpretation and the computational requirements of the evolutionary periodogram are especially considered. Finally, in Section V, we give some examples to illustrate the performance of the proposed estimator and compare our results to those obtained using the STFT, the Wigner distribution and the method of time-

Manuscript received November 21, 1991; revised June 16, 1993.
A. S. Kayhan is with the Department of Electrical and Electronics Engineering, Hecettepe University, Ankara, Turkey.
A. El-Jaroudi and L. F. Chaparro are with the Department of Electrical Engineering, University of Pittsburgh, Pittsburgh, PA 15261 USA.
IEEE Log Number 9400398.

1053-587X/94$04.00

frequency representation using cone-shaped and exponential kernels [6], [7].

II. Problem Statement

In this section, we first define a time-dependent spectral density for a nonstationary process, and then formulate the estimation of the spectral density as the estimation of a time-varying amplitude at each frequency.

A. Definitions

According to the Wold-Cramer decomposition [4], a discrete-time nonstationary process $x[n]$ can be represented as the output of a causal, linear, time-varying system with impulse response $h[n, m]$

$$x[n] = \sum_{m=-\infty}^{n} h[n,m]\varepsilon[m] \tag{1}$$

where $\{\varepsilon[m]\}$ is a stationary zero-mean, unit-variance white noise process. Furthermore, as a stationary signal $\{\varepsilon[m]\}$ may be expressed as a "sum" of sinusoids with random amplitudes and phases

$$\varepsilon[m] = \int_{-\pi}^{\pi} e^{j\omega m} dZ(\omega) \tag{2}$$

where $Z(\omega)$ is a process with orthogonal increments, i.e.

$$E\{dZ(\omega_1)dZ^*(\omega_2)\} = 0 \qquad \omega_1 \neq \omega_2 \tag{3}$$

and

$$E\{|dZ(\omega)|^2\} = \frac{d\omega}{2\pi}. \tag{4}$$

Thus, by substituting (2) into (1), we can express the nonstationary process $x[n]$ as

$$x[n] = \int_{-\pi}^{\pi} H(n,\omega)e^{j\omega n} dZ(\omega) \tag{5}$$

where

$$H(n,\omega) = \sum_{m=-\infty}^{n} h[n,m]e^{-j\omega(n-m)} \tag{6}$$

is Zadeh's generalized transfer function [16], [17] of a linear time-varying system with impulse response $h[n, m]$ and evaluated on the unit circle.

In (5), the nonstationary process is expressed as a "sum" of sinusoids with time-varying amplitudes and phases. From (5), the variance of $\{x[n]\}$ is given by

$$E\{|x[n]|^2\} = \frac{1}{2\pi}\int_{-\pi}^{\pi} |H(n,\omega)|^2 d\omega. \tag{7}$$

Equation (7) shows the distribution of the power of the nonstationary process $\{x[n]\}$ at each time n, as a function of the frequency parameter ω. Thus, the Wold-Cramer evolutionary spectrum [11] is thus defined as

$$S(n,\omega) = |H(n,\omega)|^2. \tag{8}$$

This definition was independently proposed by Tjostheim [4] and Melard [4], [11], and constitutes a special case of Priestley's evolutionary spectrum [4], [11]. Instead of a class of spectral functions, as in Priestley's general case, the Wold-Cramer evolutionary spectrum is uniquely given by the representation of the nonstationary process.

The definition in (8) can be viewed as Priestley's evolutionary spectrum if one restricts the function $H(n, \omega)$ to the class of oscillatory functions. This restriction requires these functions to be slowly-varying in time. Otherwise multiple spectra can be obtained from the same signal, and the meaning of the frequency parameter ω becomes ambiguous. Below we present a trivial example of this ambiguity.

Example: Given the signal $x[n] = 1$, for all time n, this signal can be written in the form of equation (5) as $x[n] = H(n,0)e^{j0n}$ with $H(n, 0) = 1$, which will produce a spectrum $S(n, 0) = 1$. The same signal can be written as $x[n] = H(n,\pi)e^{j\pi n}$ with $H(n,\pi) = e^{-j\pi n}$, and will have a spectrum $S(n, \pi) = 1$. Note that this one signal can be seen as having the same spectrum at various frequencies. However, only the first ($H(n, 0) = 1$) satisfies Priestley's restrictions on the function $H(n, \omega)$.

We will impose a condition similar to Priestley's on the time-varying amplitudes and we will later show how this condition relates to the work of Priestley and its effect on the time frequency resolution of the spectral estimator.

Now consider the component of $x[n]$ at frequency ω_0

$$x_0[n] = H(n,\omega_0)e^{j\omega_0 n} dZ(\omega_0). \tag{9}$$

This component is a complex exponential of frequency ω_0, with random time-varying amplitude and phase, such that its local power is given by

$$E\{|x_0[n]|^2\} = |H(n,\omega_0)|^2 \frac{d\omega_0}{2\pi} = S(n,\omega_0)\frac{d\omega_0}{2\pi}. \tag{10}$$

Hence, the average squared of this component carries the power-frequency distribution as a function of time. Priestley [4] suggests obtaining $x_0[n]$ by bandpass filtering $x[n]$ around ω_0, and then obtaining the time-varying power at ω_0 by estimating the local power in a short-time window. We present in the remainder of this paper an approach which does not require explicitly obtaining $x_0[n]$ and computes a minimum mean-squared error estimate of the time-varying amplitude.

B. Model at a Frequency ω_0

Let us model $x[n]$, when considering a frequency of interest ω_0, as

$$x[n] = x_0[n] + y_{\omega_0}[n] = A(n,\omega_0)e^{j\omega_0 n} + y_{\omega_0}[n] \tag{11}$$

where $y_{\omega_0}[n]$ is a zero-mean modeling error which includes the components of $x[n]$ at frequencies different from ω_0; and, from (9), we have defined

$$A(n,\omega_0) = H(n,\omega_0)dZ(\omega_0). \tag{12}$$

Notice that

$$E\{|A(n,\omega_0)|^2\} = S(n,\omega_0)\frac{d\omega_0}{2\pi} \tag{13}$$

and therefore, by estimating $A(n, \omega_0)$ from the data $x[n]$, we can estimate $S(n, \omega_0)$ and repeating this process for all frequencies ω, we obtain an estimate of the time-dependent spectral density $S(n, \omega)$.

Consider then the practical case in which $x[n]$ is given in a finite interval and we model it as before, i.e.

$$x[n] = A(n, \omega_0) e^{j\omega_0 n} + y_{\omega_0}[n] \qquad 0 \le n \le N-1. \quad (14)$$

Assume also that $A(n, \omega_0)$ varies with time in such a way that it can be represented as an expansion of functions $\{\beta_i[n]\}$ which are orthonormal over $0 \le n \le N-1$, i.e.

$$A(n, \omega_0) = \sum_{i=0}^{M(\omega_0)-1} \beta_i^*[n] a_i = \mathbf{b}[n]^H \mathbf{a} \quad (15)$$

where $(.)^H$ stands for the Hermitian transpose operation, $\mathbf{a} = [a_0 \cdots a_{M-1}]^T$ is a vector of the random expansion coefficients, and $\mathbf{b}[n] = [\beta_0[n] \cdots \beta_{M-1}[n]]^T$ is a vector of the orthonormal functions at time n. The number of expansion functions $M(\le N)$ depends on the frequency ω_0 and indicates the degree to which $A(n, \omega_0)$ varies with time. For small values of M, $A(n, \omega_0)$ is slowly varying, and for large values of M, it is rapidly varying. It is important to note that expressing $A(n, \omega_0)$ as a smoothly-varying function of time does not contradict the definition of $A(n, \omega_0)$ in (12). The random component $dZ(\omega_0)$ is not a function of time, and for every realization of the process $x[n]$, the $dZ(\omega_0)$ term will have but a single value. Thus $dZ(\omega_0)$ has no influence on the time behavior of $A(n, \omega_0)$.

Clearly any time behavior of $A(n, \omega_0)$ can be approximated arbitrarily closely by increasing M. Therefore for a large M, the choice of expansion functions is not critical. However, as we shall see later, large values of M adversely affect the frequency resolution of the estimator. Consequently, one should use all *a priori* knowledge available to select the set of functions best suited for the time-behavior to be approximated, so that the order of the expansion is kept at a minimum.

Based on the above assumptions for the time-varying amplitude $A(n, \omega_0)$, the signal $x[n]$ can be expressed in the following vector form

$$\mathbf{x} = \mathbf{F}\mathbf{a} + \mathbf{y} \quad (16)$$

where $\mathbf{F}$ is an $N \times M$ matrix with entries

$$\{f_{n,i}\} = \{\beta_i^*[n] e^{j\omega_0 n}\}, 0 \le n \le N-1, 0 \le i \le M-1 \quad (17)$$

and

$$\mathbf{x} = [x[0] \cdots x[N-1]]^T$$
$$\mathbf{y} = [y_{\omega_0}[0] \cdots y_{\omega_0}[N-1]]^T.$$

Based on this model, we propose below a minimum mean-squared error estimator of the time-varying amplitude $A(n, \omega_0)$.

III. Linear Estimation of $A(n, \omega_0)$

In this section we propose a linear estimator for the time-varying amplitude at a given frequency, as well as derive the conditions for it to minimize a mean-squared error measure.

A. Linear Estimator

Let us consider the following linear estimator for $A(n, \omega_0)$

$$\hat{A}(n, \omega_0) = \sum_{k=0}^{N-1} w_k^*[n] x[k] \quad (18)$$

where $w_k[n]$ are weights to be determined later. The estimator in (18) is given in vector form by

$$\hat{A}(n, \omega_0) = \mathbf{w}[n]^H \mathbf{x} \quad (19)$$

where $\mathbf{w}[n]$ is a $N \times 1$ vector with weights $\{w_k[n]\}$.

By substituting (16) into (19), we write the estimator as

$$\hat{A}(n, \omega_0) = \mathbf{w}[n]^H \mathbf{F}\mathbf{a} + \mathbf{w}[n]^H \mathbf{y}. \quad (20)$$

The equation above shows that each estimate is formed of two components: The first depends on the time-varying amplitude at the frequency of interest ω_0, and the second is an error term which depends on all the other components of $x[n]$ at frequencies different from ω_0. The optimal estimator must produce the correct time-varying amplitude from the first component and minimize the contribution of the error term. In other words, we need to impose the restrictions that

$$\mathbf{w}[n]^H \mathbf{F}\mathbf{a} = \mathbf{b}[n]^H \mathbf{a} \quad (21)$$

or

$$\mathbf{w}[n]^H \mathbf{F} = \mathbf{b}[n]^H. \quad (22)$$

Also we minimize the mean-squared error

$$\begin{aligned} \text{MSE} &= E\{|A(n, \omega_0) - \hat{A}(n, \omega_0)|^2\} \\ &= \mathbf{w}[n]^H E\{\mathbf{y}\mathbf{y}^H\} \mathbf{w}[n] \\ &= \mathbf{w}[n]^H \mathbf{R}_{yy} \mathbf{w}[n] \end{aligned} \quad (23)$$

where $\mathbf{R}_{yy}$ is the covariance matrix of the modeling error $y_{\omega_0}[n]$. Equations (22) and (23) above constitute "band-pass" type estimator conditions: Letting the desired component through unchanged and minimizing the contribution of the undesired components.

B. Mean-Squared Error Minimization

Since $y_{\omega_0}[n]$ is a function of the analysis frequency ω_0 and is not known *a priori*, we make the assumption that $\mathbf{R}_{yy} = \mathbf{I}$. In other words, we assume the modeling error is white. This assumption, while seemingly not realistic, makes the estimator suppress equally components not at the frequency of interest. This assumption is actually the most general one could make about the modeling error $y_{\omega_0}[n]$ in absence of any *a priori* information about it. It is important to note that this assumption affects only the suppression capabilities of the estimator weights, and that it is similar to the assumptions made for the periodogram estimator in the stationary case [18]. By applying this assumption to (23), the mean-squared error reduces to

$$\text{MSE} = \mathbf{w}[n]^H \mathbf{w}[n]. \quad (24)$$

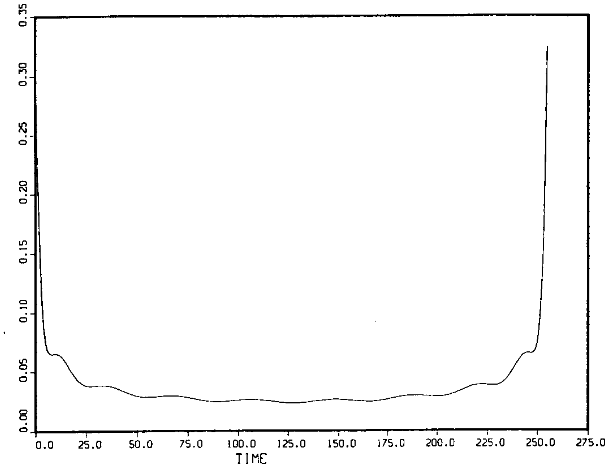

Fig. 1. Time-dependent minimum mean-squared error.

We minimize this error subject to the constraints in (21) using the method of Lagrange multipliers, i.e., we minimize the cost function

$$C[n] = \mathbf{w}[n]^H\mathbf{w}[n] - [\mathbf{w}[n]^H\mathbf{F} - \mathbf{b}[n]^H]\lambda \quad (25)$$

where λ is an $M \times 1$ vector of Lagrange multipliers. By setting the derivative of the cost function to zero, we obtain the following minimization conditions

$$\mathbf{w}_{\text{opt}}[n]^H = \lambda^H\mathbf{F}^H. \quad (26)$$

Solving for the vector λ by multiplying both sides of (26) by $\mathbf{F}$ from the right and using the property $\mathbf{F}^H\mathbf{F} = \mathbf{I}$ (due to the orthonormality of the functions $\{\beta_i[n]\}$), and the conditions in (22) we get

$$\begin{aligned}\lambda^H &= \mathbf{w}_{\text{opt}}[n]^H\mathbf{F}\\ &= \mathbf{b}^H[n].\end{aligned} \quad (27)$$

Substituting (27) into (26) to obtain the optimal weights yields

$$\mathbf{w}_{\text{opt}}[n] = \mathbf{F}\mathbf{b}[n]. \quad (28)$$

Finally, the minimum mean-squared error is obtained by substituting (28) into (24)

$$\text{MSE}_{\min} = \mathbf{b}[n]^H\mathbf{b}[n] = \sum_{i=0}^{M-1} |\beta[n]|^2. \quad (29)$$

Two observations are in order here. First, the minimum MSE varies with time and depends on the set of expansion functions selected for the analysis. Fig. 1 shows the minimum MSE as a function of time for the discrete Legendre set of orthonormal polynomials [19] with $M = 6$, and $N = 256$. Second, the optimal weights $\mathbf{w}_{\text{opt}}[n]$ do not depend on the observed data vector $\mathbf{x}$, a direct result of the white noise assumption imposed on the process $y_{\omega_0}[n]$.

The minimum MSE estimator is then obtained by substituting (28) in (19) and is given in vector form by

$$\hat{A}(n,\omega_0) = \mathbf{b}[n]^H\mathbf{F}^H\mathbf{x} \quad (30)$$

or alternatively in scalar form by

$$\hat{A}(n,\omega_0) = \sum_{i=0}^{M-1} \beta_i^*[n] \sum_{k=0}^{N-1} \beta_i[k]x[k]e^{-j\omega_0 k}. \quad (31)$$

IV. Minimum Mean-Squared Error Spectral Estimation

In this section, we define the Evolutionary Periodogram (EP) based on the minimum mean-squared error amplitude estimator developed in the previous section. We also derive and examine many properties of this spectral estimator.

A. The Evolutionary Periodogram

The estimator $\hat{A}(n,\omega_0)$ in (31) provides an estimate of the time-varying amplitude of the component of $x[n]$ at frequency ω_0; by varying ω_0 over all possible values of frequency, we obtain the time-varying amplitude $\hat{A}(n,\omega)$ for all discrete frequencies. An estimate of the time-varying spectral density is then given by

$$\begin{aligned}\hat{S}_{\text{EP}}(n,\omega) &= \frac{2\pi}{d\omega}|\hat{A}(n,\omega)|^2 &(32)\\ &= \frac{N}{M}\left|\sum_{i=0}^{M-1} \beta_i^*[n] \sum_{k=0}^{N-1} \beta_i[k]x[k]e^{-j\omega k}\right|^2 &(33)\end{aligned}$$

where we have dropped the expectation operator from the definition in (13). The factor $2\pi M/N$ substituted for $d\omega$ will be explained later in this section.

We call this estimator the evolutionary periodogram (EP). The reason for this name is twofold: (1) The derivation parallels closely the one given for the periodogram in [18], (2) for the special case where $\hat{A}(n,\omega)$ does not vary with time (i.e., $M = 1, \beta_0 = 1/\sqrt{N}$), the EP reduces to

$$\hat{S}_{\text{EP}}(n,\omega) = \frac{1}{N}\left|\sum_{k=0}^{N-1} x[k]e^{-j\omega k}\right|^2 \quad (34)$$

which is the standard periodogram spectral estimator. The proposed EP thus includes the periodogram estimator for stationary processes as a special case.

B. Properties of the EP

Many of the properties of the periodogram have their counterparts in the EP, some of which will be considered below.

Time-Frequency Resolution: The EP in (33) can be written as

$$\hat{S}_{\text{EP}}(n,\omega) = \frac{N}{M}\left|\sum_{k=0}^{N-1}\left[\sum_{i=0}^{M-1} \beta_i^*[n]\beta_i[k]\right]x[k]e^{-j\omega k}\right|^2 \quad (35)$$

which can be interpreted as the magnitude squared of the Fourier transform of $x[k]$ windowed by the sequence $v[n,k] = \sum_{i=0}^{M-1} \beta_i^*[n]\beta_i[k]$. We observe that the frequency resolution of the estimator is therefore determined by the bandwidth of the window $v[n,k]$. The Fourier transform of this time-varying window is given by

$$V(n,\omega) = \sum_{i=0}^{M-1} \beta_i^*[n] B_i(\omega) \tag{36}$$

where $B_i(\omega)$ is the Fourier transform of $\beta_i[n]$. Since $V(n,\omega)$ is a linear combination of the Fourier transforms of the N-point expansion functions $\{\beta_i[n], 0 \le i \le M-1\}$, the bandwidth of $V(n,\omega)$ is approximately equal to the highest frequency of significance in $\{B_i(\omega), 0 \le i \le M-1\}$. For many of the standard sets of expansion functions (e.g., Fourier, Legendre), this frequency $\omega_{\max}$ is approximately $2\pi(M-1)/N$ radians, and since the expansion functions are defined over N points, $\omega_{\max}$ is the center of a lobe which is $2\pi/N$ radians wide. The bandwidth of the window $V(n,\omega)$ is then $2\pi(M-1)/N + 2\pi/N = 2\pi M/N$ radians. Therefore, a frequency component in the input signal will spread (smear) with a width $2\pi M/N$, so that, frequency components which are closer than $2\pi M/N$ cannot be resolved. It is this bandwidth which is substituted for $d\omega$ in (32) above to give the form of the EP estimator in (33).

Note that for $M = 1$ (stationary processes), the bandwidth reduces to $2\pi/N$, the resolution of the periodogram, which is not surprising in the light of the earlier discussion. Also for a full set of expansion functions $M = N$, the bandwidth increases to 2π, which means that we cannot resolve any frequency components. This result illustrates that if we do not restrict the time-behavior of the amplitudes $A(n,\omega)$, i.e. if we let $M = N$, the spectrum smears over all frequencies and the estimator will yield values of the spectrum which are constant in frequency. The parameter ω then loses its physical interpretation [4]. Therefore, to obtain meaningful spectra one has to restrict the time behavior of $A(n,\omega)$ (as pointed out by Priestley [4]) by making M much smaller than N.

As we increase our ability to track fast changes in time by increasing M to include higher order basis functions, we increase the minimum separation between resolvable frequency components thereby decreasing the frequency resolution. If we decrease our resolution in time by decreasing M, we decrease the minimum separation between resolvable frequency components thereby increasing our resolution in frequency. It is important to note that, as in the STFT, the resolution can be further controlled using the length N of our analysis sequence.

The bandwidth of $V(n,\omega)$ is sometimes actually smaller than $2\pi M/N$. Recall that $V(n,\omega)$ is a linear combination of $\{B_i(\omega), 0 \le i \le M-1\}$ and that each of these functions is weighted using $\beta_i[n]$. Therefore, for certain values of n—when $\beta_{M-1}[n]$ is very small (or zero)—$B_{M-1}(\omega)$ has little or no contribution to $V(n,\omega)$. The highest frequency component in $V(n,\omega)$ is then associated with $B_{M-2}(\omega)$ and the bandwidth decreases (the frequency resolution increases) by a factor of $2\pi/N$. Hence, depending on the set of expansion functions used, the EP achieves better frequency resolutions at certain times than at others.

In Fig. 2(a), we show a plot of $|V(n,\omega)|^2$ for $N = 64$ and $M = 2$ where we used the discrete Legendre polynomials for our basis functions. Note how the bandwidth of $V(n,\omega)$ varies with time. It is narrowest for $n = 31$, and 32 and widest for $n = 0$, and 63. In Fig. 2(b), the solid line shows the window at its narrowest bandwidth, and the dashed line shows the window at its widest bandwidth.

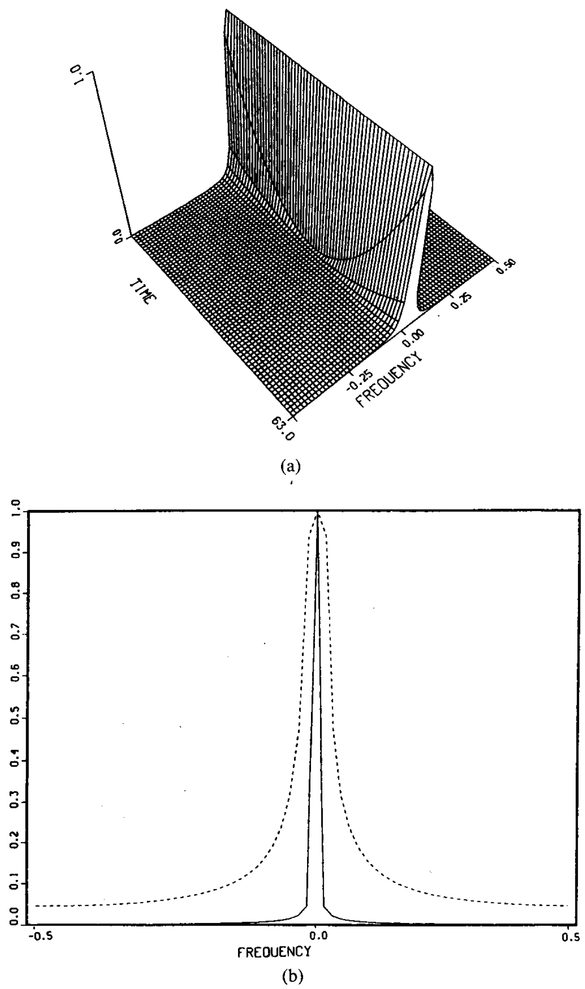

Fig. 2. (a) Fourier transform of the window function. (b) Bandwidth of window at its narrowest point (solid line) and widest point (dashed line).

It is also important to recall that the parameter M can be a function of frequency allowing us to tailor the resolution in time-frequency to suit the task at hand.

Filtering Interpretation of the EP: The EP estimator in (33) at a certain frequency ω_0 can also be written as

$$\hat{S}_{\mathrm{EP}}(n,\omega_0) = \frac{N}{M}\left|\sum_{k=0}^{N-1}\left[\sum_{i=0}^{M-1}\beta_i^*[n]\beta_i[k]\right]x[k]\right|^2 = \frac{N}{M}\left|\sum_{k=0}^{N-1} g[n,\ell-k]x[k]\right|^2_{\ell=0}. \tag{37}$$

Therefore, $\hat{S}_{\mathrm{EP}}(n,\omega_0)$ can be considered as the magnitude squared of the output of a linear time-varying filter with a

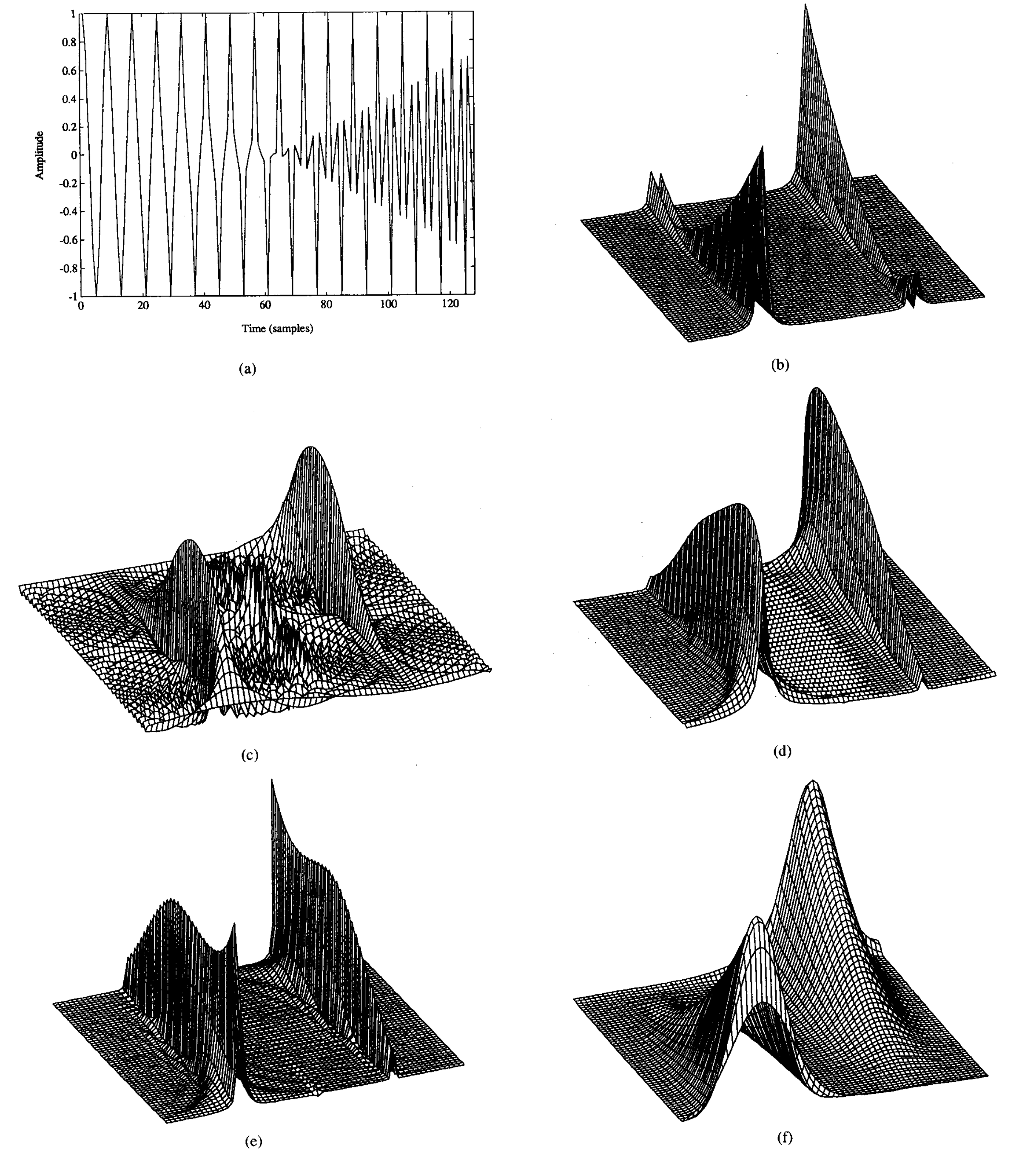

Fig. 3. (a) Real part of signal in example 1. (b) EP estimate for signal in example 1. (c) Wigner distribution for signal in example 1. (d) Time-frequency representation with cone-shaped kernels for signal in example 1. (e) Time-frequency representation with exponential kernels for signal in example 1. (f) The STFT estimate for signal in example 1.

finite time-dependent impulse response

$$g[n,k] = \begin{cases} \sum_{i=0}^{M-1} \beta_i^*[n]\beta_i[-k]]e^{j\omega_0 k}, & -(N-1) \leq k \leq 0 \\ 0, & \text{otherwise} \end{cases}$$

and excited with an input $x[n]$. This is a bandpass filter with time-varying frequency response centered around ω_0

$$G(n,\omega) = \sum_{i=0}^{M-1} \beta_i^*[n] B_i(\omega - \omega_0). \tag{38}$$

Computing $\hat{S}_{\mathrm{EP}}(n,\omega_0)$ is thus equivalent to passing $x[n]$

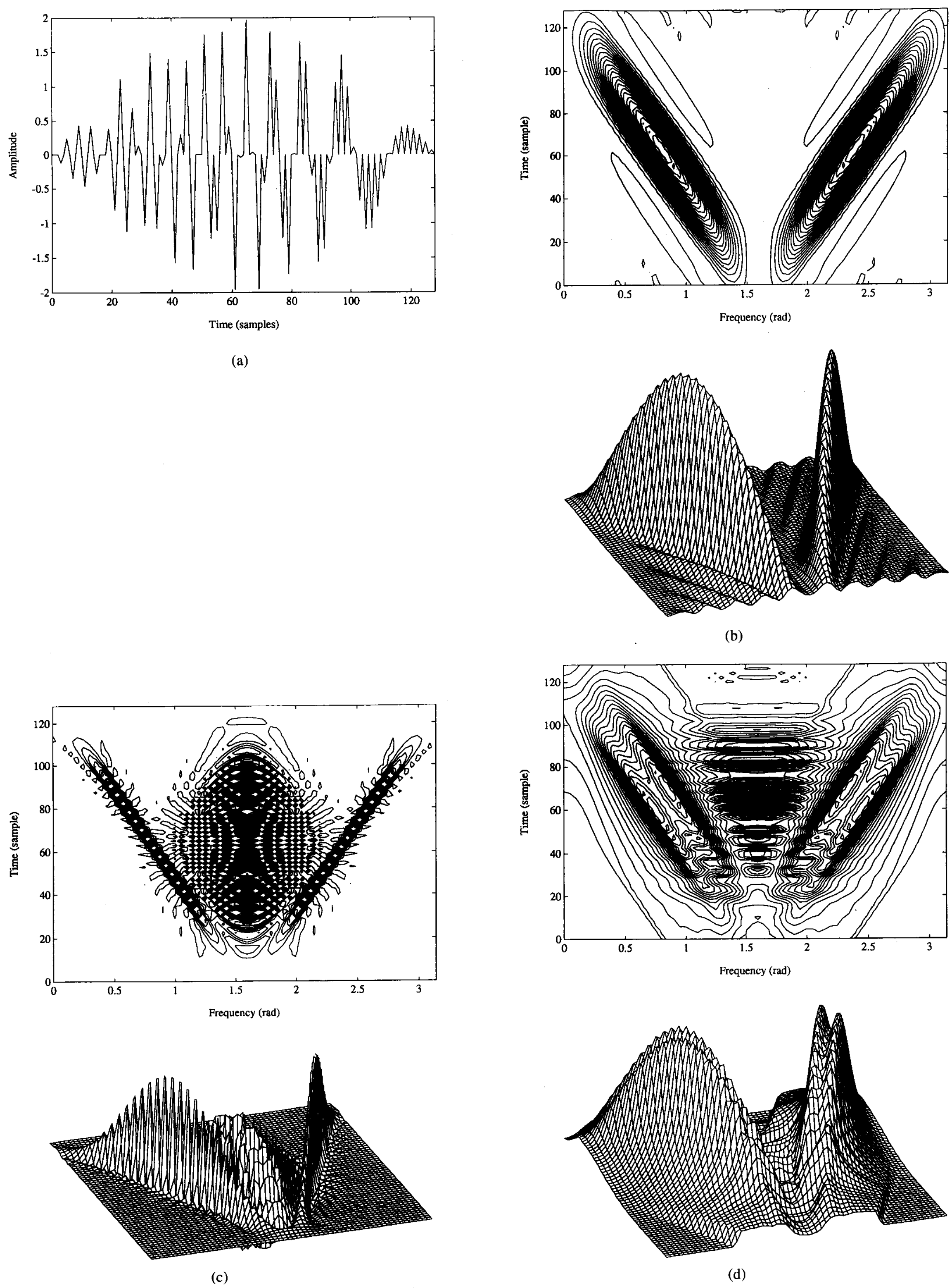

Fig. 4. (a) Real part of signal in example 2. (b) EP estimate for signal in example 2. (c) Wigner distribution for signal in example 2. (d) Time-frequency representation with cone-shaped kernels for signal in example 2.

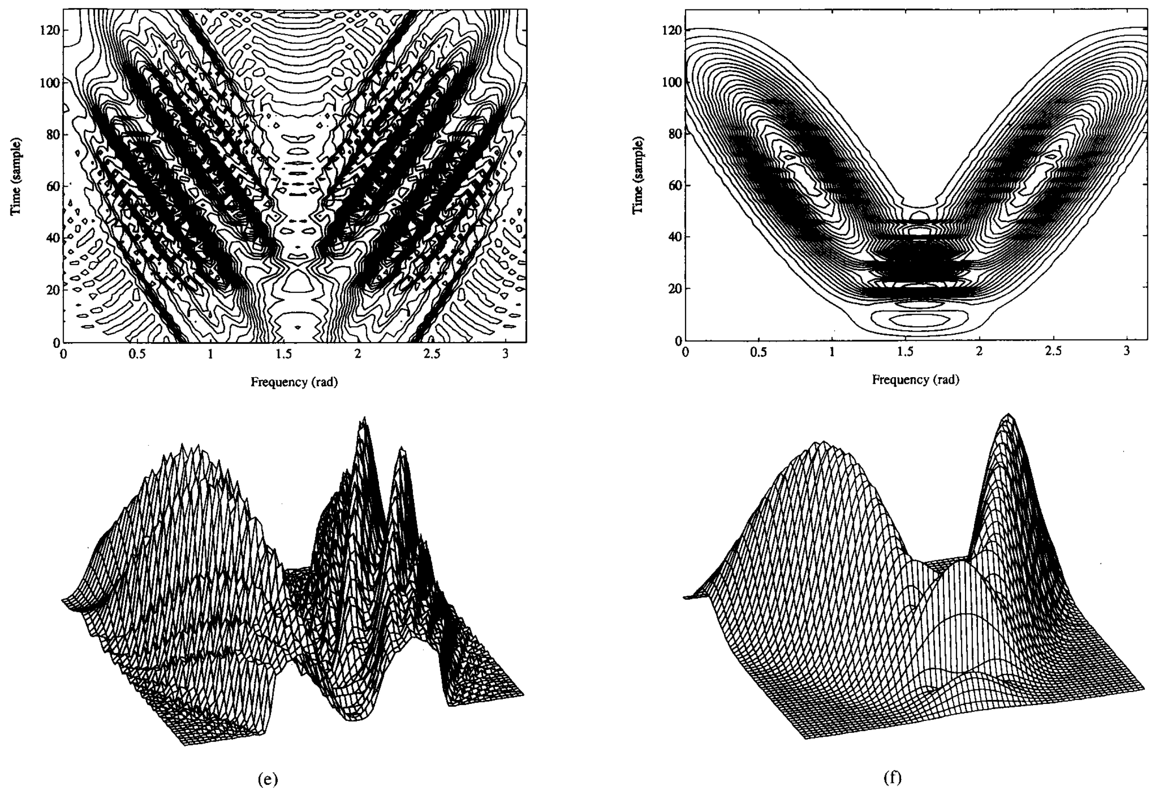

Fig. 4. *(continued)* (e) Time-frequency representation with exponential kernels for signal in example 2. (f) The STFT estimate for signal in example 2.

through a time-varying bandpass filter centered around the frequency of interest, and then computing the local energy of the output by calculating its magnitude squared. This property has a well-known equivalent for the periodogram [18] and for the STFT [8] estimators.

It is worthwhile to point out that the filtering interpretation shows the similarity of the EP to the process suggested by Priestley [4] for computing the evolutionary spectrum. However, the approach to obtain the EP differs from Priestley's in the following points. First, the EP bandpass filters are time-varying and designed using the set of orthonormal functions that constrain the time behavior of the spectral density. Second, this approach is computationally efficient as we shall see below. Third, there is no time-averaging in computing the local power in contrast to Priestley's approach.

Computational Requirements of the EP: The EP estimate can be computed efficiently over a finite interval $0 \leq n \leq N-1$ by using fast Fourier transform (FFT) algorithms (if M is constant for all frequencies). We use M FFT's to calculate the inner summation in (33)—the Fourier transform of $\beta_i[k]x[k]$, for $0 \leq i \leq M-1$. Then, at each time n we calculate the weighted summation of these values. Therefore, the computational load is directly proportional to the number of expansion functions. For M expansion functions over N samples, we perform $N \times M$ complex multiplications to calculate $\beta_i[k]x[k]$ (assuming the functions are complex), $M \times N \log_2 N$ complex multiplications and additions for the FFTs, and $2M \times N^2$ complex multiplications and additions to combine these values into an amplitude estimate. Thus, $M(2 + (\log_2 2N)/N)$ complex multiplications and additions are necessary for each sample in the time-frequency plane before the calculation of the magnitude squared. It is possible to use parallel processors for real time applications of the EP with delay.

V. Examples

In this section we present simulation results using the EP estimator, and compare them with results using the Wigner distribution, the short-time Fourier transform, and the time-frequency distribution using the cone-shaped kernel and the exponential kernel.

For the first example, the signal is given by

$$x_1[n] = A_1[n]e^{j\omega_1 n} + A_2[n]e^{j\omega_2 n} \tag{39}$$

where $A_1[n] = 1 - n/(N-1)$, $A_2[n] = n/(N-1)$, $\omega_1 = 0.3\pi$, $\omega_2 = 0.7\pi$, and $N = 128$. The signal is composed of two sinusoids: One with a linearly increasing amplitude, and the other with a linearly decreasing amplitude. The real part of this signal is shown in Fig. 3(a). The EP estimate is shown in Fig. 3(b), the Wigner distribution (WD) in Fig. 3(c), the estimate using the cone-shaped kernel (CSK) for time-frequency representation [6] in Fig. 3(d), the one

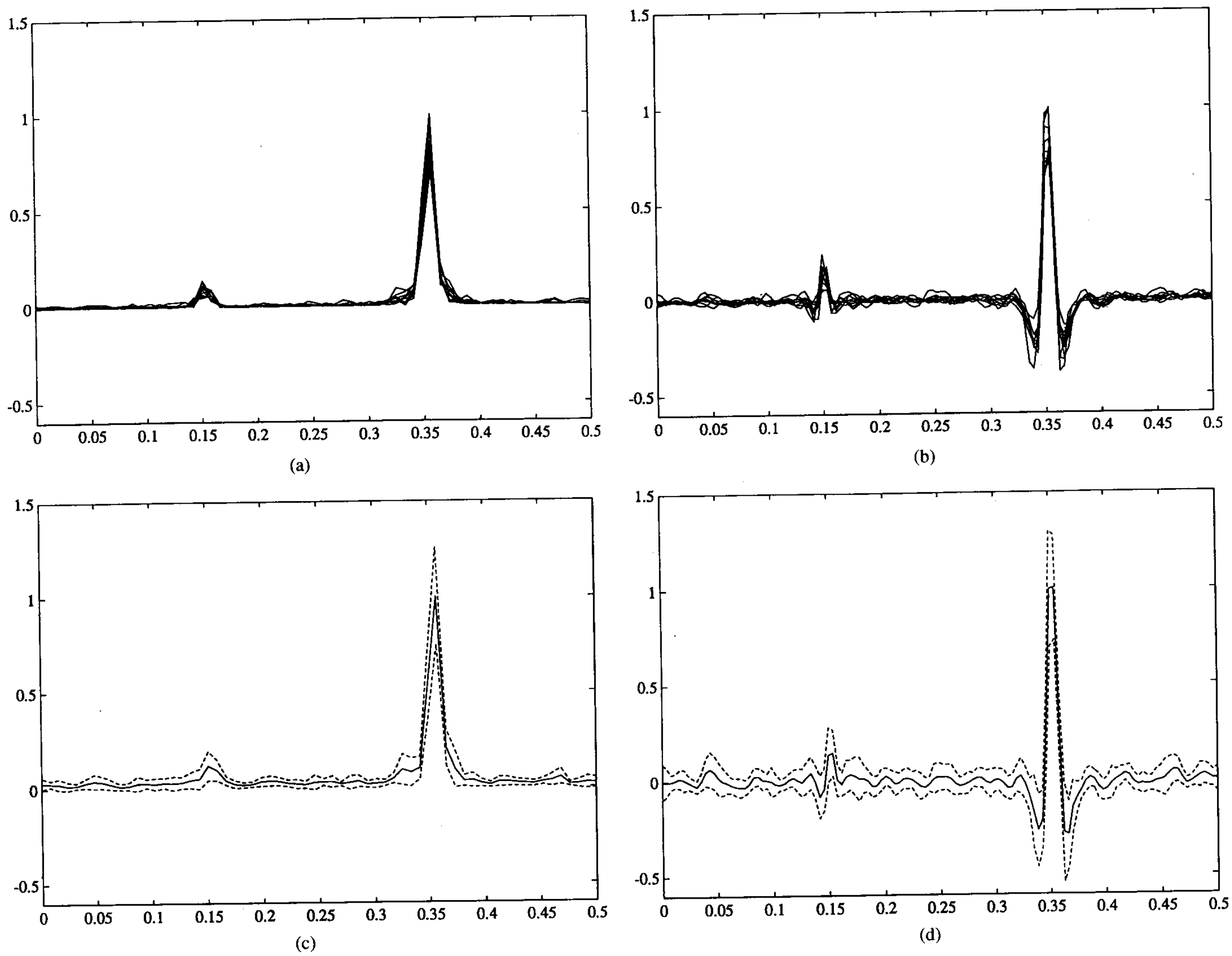

Fig. 5. EP spectral estimate at time n = 32 for sinusoids in noise in example 3. (b) Spectral estimate at time n = 32 for sinusoids in noise in example 3 using time-frequency representation with cone-shaped kernels. (c) Average (solid line) plus/minus one standard deviation (dashed line) of the EP spectral estimates in example. (d) Average (solid line) plus/minus one standard deviation (dashed lines) of the time-frequency representation with cone-shaped kernels estimates in example 3.

using the exponential kernels (EK) [7] in Fig. 3(e), and the STFT in Fig. 3(f). For the EP, we use the discrete Legendre polynomials with $M = 2$. For the CSK, we use a cone parameter $c = 0.000143$, for the STFT a Hamming window of length 16, and for the EK, the parameter $\sigma = 1$. Clearly, the EP estimate is superior to its counterparts. Fig. 3(b) clearly shows the quadratic time behavior of the power in each sinusoid, and displays no cross-term behavior and a strictly nonnegative estimate. Fig. 3(c) shows the cross-terms of the Wigner distribution, which overwhelm the true components of the signal. The WD, CSK and EK display negative estimates. The EP also outperforms the STFT by tracking the time behavior more accurately with better frequency resolution.

In the second example, the signal is given by

$$x_2[n] = A[n](e^{j\omega_1[n]n} + e^{j\omega_2[n]n}) \tag{40}$$

where $A[n] = 16n(N-n)/N^2$, $\omega_{1,2}[n] = \pi/2 \pm \pi n/4N$ and $N = 128$. This signal is a sum of 2 chirps with quadratic amplitudes, one with increasing frequency and one with decreasing frequency. Fig. 4(a) shows the real part of this signal. Fig. 4(b) illustrates the EP estimate, Fig. 4(c) the Wigner distribution, Fig. 4(d) the CSK estimate, Fig. 4(e) the EK estimate, and Fig. 4(f) the STFT. For each estimate, we display the 3-D mesh plot of the time-frequency distribution and a 2-D contour plot of the same. In this case, we use the set of Fourier basis functions with $M = 5$ for the EP, and the same parameters as in the previous example for the other estimators. Again, the WD, CSK, and EK produce undesired cross-terms and negative estimates. Also, by comparing the contour plots, it is clear that the EP produces better time-frequency resolution than the STFT.

In the third example, we demonstrate the performance of the EP in noisy environments. We use the signal in the first example and imbed it in white Gaussian noise. Fig. 5(a) shows the EP estimate with $M = 2$ at time $n = 32$ for ten different seeds with SNR = 25 dB. Fig. 5(b) shows the estimate produced by the method of time-frequency representation using cone-shaped kernels (CSK) for the same

n and the same seeds. The EP produces better estimates which clearly show the two sinusoids in the signal while the other approach produces estimates with negative values and large spurious peaks. Figs. 5(c) and 5(d) show the average of the ten estimates (solid line) plus/minus one standard deviation (dashed lines) with SNR $=$ 19 dB for the EP and CSK, respectively. The EP is clearly the approach with the lower variance and the advantage of nonnegative estimates.

VI. Conclusion

In this paper, we propose a novel approach for the estimation of the spectra of nonstationary signals. This approach, which we call the evolutionary periodogram is based on expressing the time-varying amplitude at each frequency as an expansion of orthonormal functions, then obtaining a minimum mean-squared estimate of these amplitudes. The EP has the standard periodogram estimator as a special case. We examine the time-frequency resolution trade-off properties of the EP, its filtering interpretation and its computational advantages. The EP outperforms the Wigner distribution and the STFT in analyzing nonstationary signals. It produces estimates which are easily interpreted and does not suffer from the drawbacks of current approaches.

References

[1] R. M. Loynes, "On the concept of the spectrum for nonstationary processes," *J. Royal Statistical Soc., Ser. B*, vol. 30, no. 1, pp. 1–30, 1968.

[2] J. B. Allen and L. R. Rabiner, "A unified theory of short-time spectrum analysis and synthesis," *Proc. IEEE*, vol. 65, no. 11, pp. 1158–1564, Nov. 1977.

[3] T. A. C. M. Claasen and W. F. G. Mecklenbrauker, "The Wigner distribution—A tool for time-frequency signal analysis," *Phillips J. Res.*, vol. 35, no. 4, pp. 276–300, 1980.

[4] M. B. Priestley, *Non-Linear and Nonstationary Time Series Analysis.* London: Academic, 1988.

[5] L. Cohen, "Time-frequency distributions—A review," *Proc. IEEE*, vol. 77, no. 7, pp. 941–981, July 1989.

[6] Y. Zhao, L. E. Atlas, and I. R. J. Marks, "The use of cone-shaped kernels for generalized time-frequency representation of nonstationary signals," *IEEE Trans. Acoust., Speech, Signal Processing*, vol. 38, no. 7, pp. 1084–1091, July 1990.

[7] H. I. Choi and W. J. Williams, "Improved time-frequency representation of multicomponent signals using exponential kernels," *IEEE Trans. Acoust., Speech, Signal Processing*, vol. 37, no. 6, pp. 862–871, June 1989.

[8] L. R. Rabiner and R. W. Schafer, *Digital Processing of Speech Signals.* Englewood Cliffs, NJ: Prentice-Hall, 1978.

[9] M. R. Portnoff, "Time-frequency representation of digital signals based on short-time fourier analysis," *IEEE Trans. Acoust., Speech, Signal Processing*, vol. 28, no. 1, pp. 55–69, Feb. 1980.

[10] D. L. Jones and T. W. Parks, "A high resolution data-adaptive time-frequency representation," *IEEE Trans. Acoust., Speech, Signal Processing*, vol. 38, no. 12, pp. 2127–2135, Dec. 1990.

[11] G. Melard and A. H. Schutter, "Contributions to evolutionary spectral theory," *J. Time Series Anal.*, vol. 10, no. 1, pp. 41–63, 1989.

[12] S. T. Rao, "The fitting of nonstationary time-series models with time-dependent parameters," *J. Royal Statist. Soc., Ser. B*, 1970.

[13] Y. Grenier, "Time-dependent ARMA modeling of nonstationary signals," *IEEE Trans. Acoust., Speech, Signal Processing*, vol. 31, no. 4, pp. 899–911, Aug. 1983.

[14] M. Kahn, L. F. Chaparro, and E. W. Kamen, "Frequency analysis of nonstationary signal models," in *Proc. Conf. Inform. Sci., Syst.* (Baltimore, MD), Mar. 1988, pp. 617–622.

[15] G. Kitagawa and W. Gersch, "A smoothness priors time-varying ar coeffient modelling of nonstationary covariances time series," *IEEE Trans. Automat. Contr.*, vol. 30, no. 1, pp. 48–56, Jan. 1985.

[16] N. Huang and J. K. Aggarwall, "On linear shift-variant digital filters," *IEEE Trans. Circuits, Syst.*, vol. 27, no. 8, pp. 672–679, Aug. 1980.

[17] E. Jury, *Theory and Application of the z-Transform Method.* New York: Wiley, 1964.

[18] S. M. Kay, *Modern Spectral Estimation.* Englewood Cliffs, NJ: Prentice-Hall, 1988.

[19] C. P. Neuman and D. I. Schonbach, "Discrete (Legendre) orthogonal polynomials," *Int. J. Num. Meth. Eng.*, 1974.

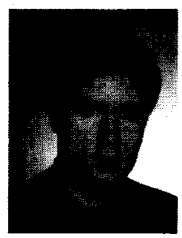

A. Salim Kayhan (S'88–M'91) was born in Turkey in 1961. He received the B.S. degree from the Midle East Technical University, Ankara, Turkey in 1985, the M.S. and Ph.D. degrees from the University of Pittsburgh in 1988 and 1991, respectively, all in electrical engineering.

Currently he is an Assistant Professor in the Department of Electrical and Electronics Engineering at Hacettepe Univerity, Ankara, Turkey. His current research interests include speech recognition, time-varying signal processing and time—frequency methods.

Amro El-Jaroudi (S'85–M'88) was born in Cairo, Egypt in 1963. He received the B.S. degree in 1984, the M.S. degree in 1984, and the Ph.D. degree in 1988, all in electrical engineering from Northeastern University, Boston, Massachusetts.

Currently he is an Assistant Professor in the Electrical Engineering Department, University of Pittsburgh, Pittsburgh, PA. His research interests include spectral estimation, digital signal processing algorithms, and speech processing. He is also an Associate Editor of the IEEE Transactions on Speech and Audio Processing.

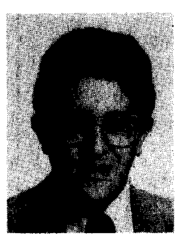

Luis F. Chaparro (S'76–M'79–SM'80) was born in Sogamoso, Colombia, in 1947. He received the B.S. degree in electrical engineering from Union College, Schenectady, NY, in 1971, and the M.S. and Ph.D. degrees in electrical engineering and computer science from the University of California at Berkeley, in 1972 and 1980, respectively.

From 1973 to 1975 he taught at the Department of Electrical Engineering, Universidad Nacional, Bogota, Colombia. Since 1979 he has been with the Department of Electrical Engineering, University of Pittsburgh, Pittsburgh, PA, where he is currently Associate Professor. His present research activities focus on statistical signal processing, multidimensional systems theory and image processing.

Dr. Chaparro is a member of the Statistical Signal and Array Processing technical committee, Tau Beta Pi, Etta Kappa Nu, and Sigma Xi.